

REFERENCES

- Akella, P.N. and Cutkosky, M.R. (1995). Contact transition control with semiactive soft fingertips. IEEE Trans. Robotics Automat., 11(6), 859-867.
- Akhavan, J. and Slack, K. (2001). Coating of a semi-conducting polymer for use in electrorheological fluids. Synt. Met., 124, 363-371.
- Askeland, D.R. (1996) The Science and Engineering of Materials, Chapman&Hall, London, p.663.
- Block, H., Kelly, J.P., Qin, A., and Watson, T. (1990). Materials and mechanism in electrorheology. Langmuir, 6, 6-14.
- Bohon, K. And Krause, S. (1998). An electrorheological fluid and siloxane gel based electromechanical actuator: working toward an artificial muscle. J. Polym. Sci. B., 36, 1091-1094.
- Brady, J.F. and Bossis, G. (1988). Stokesian dynamics. Ann. Rev. Fluid Mech., 20, 111-157.
- Cao, Y., Andreatta, A., Heeger, A.J., and Smith, P. (1989). Influence of chemical polymerization conditions on the properties of polyaniline. Polymer, 30, 2305-2311.
- Chin, B.D. and Winter, H.H. (2002). Field-induced gelation, yield stress, and fragility of an electro-rheological suspension. Rheol. Acta., 41, 265-275.
- Chin, B.D., Lee, Y.S., and Park, O.O. (1998). Effect of conductivity and dielectric behavior on the electrorheological response of a semiconductive poly(p-phenylene) suspension. J. Colloid Interface Sci., 201, 172-179.
- Cho, M.S., Lee, J.H., Choi, H.J., Ahn, K.H., and Lee, S.J. (2004). Linear viscoelasticity of semiconducting polyaniline based electrorheological suspensions. J. Mater. Sci., 39, 1377-1382.
- Choi, H.J., Cho, M.S., and To, K. (1998). Electrorheological and dielectric characteristics of semiconductive polyaniline-silicone oil suspensions. Physica A., 254, 272-279.
- Choi, S.B., Choi, Y.T., Chang, E.G., Han, S.J., and Kim, C.S. (1998). Control characteristics of a continuously variable ER damper. Mechatronics, 8, 143-161.

- Chotpattananont, D., Sirivat, A., and Jamieson, A. M. (2004). Scaling of yield stress of polythiophene suspensions under electric field. Macromol. Mat. Eng., 289, 434-441.
- Chotpattananont, D., Sirivat, A., and Jamieson, A.M. (2003). Electrorheological properties of perchloric acid-doped polythiophene suspensions. Colloid Polym. Sci., 282, 357-365.
- Chotpattananont, D., Sirivat, A., and Jamieson, A.M. (2006). Creep and recovery behaviors of polythiophene-based electrorheological fluid. Polymer 47, 3568-3575.
- Cross, L.C. (1996). Ferroelectric materials for electromechanical transducer applications. Mater. Chem. Phys. 43, 108-115.
- Dassanayake, U., Fraden, S., and Blaaderen, A.V. (2000). Structure of electrorheological fluids. J. Chem. Phys., 12(8), 3851-3858.
- Davis, L.C. (1992). Polarization forces and conductivity effects in electrorheological fluids. J. App. Phys., 72, 1334-1340.
- Furukawa, T. (1997). Structure and functional properties of ferroelectric polymers. Adv. Colloid Interface Sci., 71-72, 183-208.
- Furukawa, Y., Ueda, F., Hyodo, Y., Harada, I., Nakajima, T. and Kawagoe, T. (1988). Vibration spectra and structure of polyaniline. Macromolecules, 21, 1297-1305.
- Gow, C. J. and Zukoski, C. F. (1990). The electrorheological properties of polyaniline suspensions. J. Coll. Interf. Sci., 136, 175-188.
- Gozdalik, A., Wycislik, H., and Plochanski, J. (2000). Electrorheological effect in suspensions of polyaniline. Synt. Met., 109, 147-150.
- Han, Y.M., Lim, S.C., Lee, H.G., Choi, S.B., and Choi, H.J. (2003). Hyteresis identification of polymethylaniline-based ER fluid using Preisach model. Meter. Design, 24, 53-61.
- Hiamtup, P., Sirivat, A., and Jamieson, A.M. (2006). Electrorheological properties of polyaniline suspensions: field-induced liquid to solid transition and residual gel structure. J. Colloid. Interf. Sci., 295, 270-278
- Huang, W.S. and MacDiarmid, A.G. (1993). Optical properties of polyaniline. Polymer, 34, 1833-1845.

- Jang, W.H., Kim, J.W., Choi, H.J., and Jhon, M.S. (2001). Synthesis and electrothology of camphorsulfonic acid doped polyaniline suspensions. Colloid. Polym. Sci., 279, 823-827.
- Kamath, G.M. and Wereley, N.M. (1997). A nonlinear viscoelastic-plastic model for electrorheological fluids. Smart Mater. Struct., 6, 351-359.
- Ketz, R., Prudhomme, R. K. and Graessley, W. W. (1988). Rheology of concentrated microgel solutions. Rheol. Acta, 27, 531-539.
- Kim, S.G., Kim, J.W., Choi, H.J., Suh, M.S., Shin, M.J., and Jhon, M.S. (2000). Synthesis and electrorheological characterization of emulsion-polymerized dodecylbenzenesulfonic acid doped polyaniline-based suspensions. Coll. Polym. Sci., 278, 894-898.
- Klingenberg, D. J. Swol, F. V. and Zukoski, C. F. (1991). The small shear rate response of electrorheological suspensions. 1 Simulation in the point-dipole limit. J. Chem. Phys., 94, 6160-6169.
- Klingenberg, D.J. (1993). Simulation of the dynamic oscillatory response of electrorheological suspensions: demonstration of relaxation mechanism. J. Rheol., 37, 199-214.
- Klingenberg, D.J., Zukoski, C.F., and Hill, J.C. (1993). Kinetics of structure formation in electrorheological suspensions. J. Appl. Phys., 73, 4644-4648.
- Koul, S., Chandra, R., and Dhawan, S.K. (2000). Conducting polyaniline composite for ESD and EMI at 101 GHz. Polymer, 41, 9305-9310.
- Krause, S. and Bohon, K. (2001). Electromechanical response of electrorheological fluids and poly(dimethylsiloxane) networks Macromolecules, 34, 7179-7189.
- Lee, H.-J., Byung, D.C., Yang, S.-M., and Park, O.O. (1998). Surfactant effect on the stability and electrorheological properties of polyaniline particle suspension. J. Colloid. Interface. Sci., 206, 424-438.
- Lee, Y.H., Kim, C.A., Jang, W.H., Choi, H.J., and Jhon, M. (2001). Synthesis and electrorheological characteristics of microencapsulated polyaniline particles with melamine-formaldehyde resins. Polymer, 42, 8277-8283.
- Lengalova, A., Pavlinek, V., Saha, P., Quadrat, O., Stejskal, J. (2003). The effect of dispersed particle size and shape on the electrorheological behavior of suspensions. Euro. Polym. J., 39, 641-648.

- Li, L. and Aoki, Y. (1997). Rheological images of poly(vinyl chloride) gels. 1. The dependence of sol-gel transition on concentration. Macromolecules, 30, 7835-7841.
- Li, W. and Wan, M. J. (1999). Stability of polyaniline synthesized by a doping-dedoping-redoping method. Appl. Polym. Sci., 71, 615-621.
- Li, W.H., Du, H., Chen, G. and Yeo, S.H. (2002). Experimental investigation of creep and recovery behaviors of magnetorheological fluids. Mater. Sci. Engr., A333, 368-376.
- Liu, B. and Shaw, M.T. (2001). Electrorheology of filled silicone elastomers. J. Rheol., 45(3), 641-657.
- Luzny, W. and Banka, E. (2000). Relation between the structure and electric conductivity of polyaniline protonated with camphorsulfonic acid. Macromolecules, 33, 425-429.
- Marshall, L., Zukoski IV, C.F., and Goodwin, J.W. (1989). Effects of electric field on the rheology of non-aqueous concentrated suspensions. J. Chem. Soc. Faraday Trans.1, 85, 2785-2795.
- Mcleish, T.C.B., Jordan, T., Shaw, M.T. (1991). Viscoelastic response of electrorheological fluids I. Frequency dependence. J. Rheol., 35(3), 427-448.
- Melrose, J.R. (1992). Brownian dynamics simulation of dipole suspensions under shear: the phase diagram. Molecular Phys., 76(3), 635-660.
- Mitsumata, T., Sugitani, K., and Koyama, K.(2004). Electrorheological response of swollen silicone gels containing barium titanate. Polymer, 45, 3811-3817.
- Mzenda, V.M., Goodman, S.A., Auret, F.D., and Prinsloo, L.C. (2002). Characterization of electrical charge transfer in conductive polyaniline over the temperature range $300 < T(K) < 450$. Synt. Met., 127, 279-283.
- Otsubo, Y. and Edamura, K. (1994). Creep behavior of electrorheological fluids. J. Rheol., 38(6), 1721-1733.
- Pan, X.D. and McKinley, G.H. (1997). Structural limitation to the material strength of electrorheological fluids. Appl. Phys. Lett., 71(3), 333-335.
- Papadopoulos, C.A. (1998). Breaks and clutches using ER fluids. Mechatronics, 8, 719-726.

- Parthasarathy, M. and Klingenberg, D. J. (1996). Electrorheology: mechanisms and models. Mater. Sci. Eng., R17, 57-103.
- Pinto, N.J., Acosta, A.A., Sinha, G.P., and Aliev, F.M. (2000). Dielectric permittivity study on weakly doped conducting polymers based on polyaniline and its derivatives. Syn. Met., 113,77-81.
- Sakurai, R., See, H., Saito, T., and Sumita, M.(1999). Effect of matrix viscoelasticity on the electrorheological properties of particle suspensions. J. Non-Newtonian Fluid Mech., 81, 235-250.
- Shiga, T. (1997). Deformation and viscoelastic behavior of polymer gels in electric fields. Adv. Polym. Sci. 137, 131-163.
- Shiga, T., Ohta, T., Hirose, Y., Okada, A., and Kurauchi, T. (1993). Electroviscoelastic effect of polymeric composites consisting of polyelectrolyte particles and polymer gel. J. Mater. Sci., 28, 1293-1299.
- Shiga, T., Okada, A., and Kurauchi, T. (1993). Electroviscoelastic effect of polymer blends consisting of silicone elastomer and semiconducting polymer particles. Macromolecules, 26, 6958-6963.
- Shiga, T., Okada, A., and Kurauchi, T. (1995). Electroviscoelastic effect of doped poly(3-hexylthiophene) J. Mater. Sci. Lett., 14, 514-515.
- Sim, I.S., Kim, J.W., Choi, H.J., Kim, C.A., and Jhon, M.S. (2001). Preparation and electrorheological characteristics of poly(p-phenylene)-based suspensions. Chem. Mater., 13, 1243-1247.
- Stejskal, J. and Gilbert, R.G. (2002) Polyaniline. Preparation of a conductive polymer. Pure Appl. Chem., 74, 857-867.
- Tao, R. and Sun, J.M. (1991). Three-dimensional structure of induced electrorheological solid. Phys. Rev. Lett., 67, 398-438.
- Trilica, J., Saha, P., Quadrat, O., and Stejskal, J. (2000). Electrorheology of polyaniline-coated silica particles in silicone oil. J. Phys.D: Appl. Phys., 33, 1773-1780.
- Varga, Z., Filipcsei, G., Szilagyi, A., and Zrinyi, M. (2005). Electric and magnetic field-structured smart composites. Macromol. Symp., 227, 123-133.
- Winslow, W.M. (1949). Induced fibrillation of suspensions. J. Appl Phys., 20, 1137-1140.

- Winter, H. H. and Chambon, F. (1986). Analysis of linear viscoelasticity of a crosslinking polymer at the gel point. J. Rheol., 30, 367-382.
- Wu, C.W. and Conrad, H. (1996). A modified conduction model for the electrorheological effect. J. Phys. D: Appl. Phys., 29, 3147-3153.
- Yanju, L., Hejun, D., and Dianfu, W. (2001). ER fluid based on inorganic/polymer blend particles and its adaptive viscoelastic properties. Colloid. Surf., A189, 203-210.
- Zeng, X.-R. and Ko, T.-M. (1998). Structures and properties of chemically reduced polyanilines. Polymer, 39, 1187-1195.
- Zrinyi, M., Feher, J. and Filipcsei, G. (2000). Novel gel actuator containing TiO₂ particles operated under static electric field. Macromolecules, 33(16), 5751-5753.

APPENDICES

Appendix A The FTIR Spectrum of Polyaniline

Infrared spectra were recorded using a FT-IR spectrometer (Bruker, FRA 106/S) in the wave number range of 400-4000 cm^{-1} using the absorbance mode with 32 scans with the wavenumber resolution of $\pm 4 \text{ cm}^{-1}$. The KBr technique was used to prepare the powder samples. Specimens of the synthesized un-doped and CSA-doped polyaniline in powder form at each N_A/N_{EB} ratio were prepared by grinding the specimens with KBr powder. The mixture was recorded by using KBr as a background. The FT-IR spectra were used to identify the characteristic functional groups of the sample in order to compare with those in literature.

The FT-IR spectra of undoped and PANI-CSA were analyzed and the peak location as well as their interpretations were identified and the summarized data are shown on Table A1. In Figure A1, five characteristic peaks of emeraldine base and doped polyaniline were observed at 826, 1163, 1307, 1495, and 1584 cm^{-1} . These peaks are attributed to the out-of-plane bending vibration of C-H on para-disubstituted rings, characteristic vibrational mode of $\text{N}=\text{quinoid segment}=\text{N}$, stretching vibration of C-N, stretching vibration of N-benzoid segment $-\text{N}$, and stretching vibration of $\text{N}=\text{quinoid segment}=\text{N}$, respectively (Zeng and Ko, 1998). The PANI-CSA FT-IR spectra shows two additional absorbance peaks at 1730 and 1037 cm^{-1} due to stretching of the C=O group and the sulfonic acid salt group, respectively.

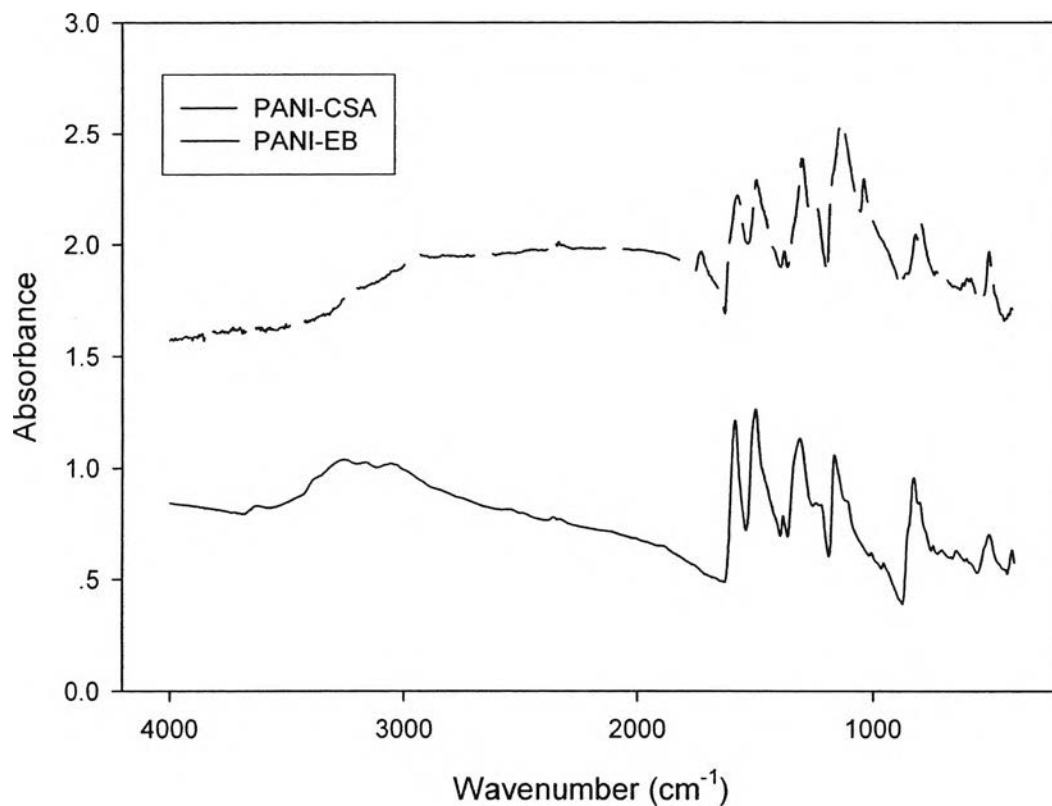


Figure A1 FT-IR spectra of undoped and PANI-CSA.

Upon doping, the relative intensity of the peaks at 1480 and 1590 cm^{-1} (1490 and 1584 in this present case), I_{1480}/I_{1590} , reflects the content of the para-disubstituted benzene ring and quinone diimine structure (Furakawa et al, 1988).

Table A1 Assignment peaks for FT-IR absorption bands of doped and CSA-doped polyanilines

Wavenumber (cm ⁻¹)		Assignments	References
PANI	PANI-CSA		
3290 ± 3		Stretching of hydrogen bond N-H	Zheng et al. (1997)
	1730 ± 2	Stretching of C=O group of acid	The Aldrich library of FT-IR spectra
1584	1575 ± 1	Stretching of N=Q=N	Wan and Li (1996)
1495	1491 ± 1	Stretching of N-B-N	Zeng and Ko (1998)
1378	1373	Stretching of C-N (QB ^t Q)	Lee et al. (2000)
1307	1297	Stretching of C-N(QB ^c Q, QBB, BBQ)	Lee et al. (2000)
1163 ± 1	1132 ± 1	Characteristic vibrational mode of N=Q=N	Zeng and Ko (1998)
	1037 ± 1	Sulfonic acid salt group	The Aldrich library of FT-IR spectra
826	798	Out-of-plane bending of C-H of paradisubstituted ring	Jang et al. (2001)

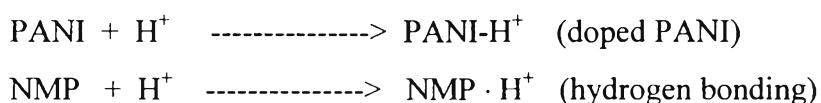
From Table X.1, Q = quinoid unit; B = benzenoid unit; B^t = trans benzenoid unit, B^c = cis benzenoid unit.

Appendix B The UV-Visible Spectra of Polyaniline

UV-visible spectra were recorded with a UV-Visible (UV-Vis, Shimadzu, UV2550). Measurements were taken in the absorbance mode in the wavelength range of 300-900 nm. Samples of emeraldine base and CSA-doped PANI solution were prepared by in different solvent, NMP for emeraldine base and chloroform for doped PANI, at the concentration of 0.05 g/L and each sample was put in a quartz cell and the UV-visible spectra were recorded by using NMP and chloroform as a background. UV-visible spectra were analyzed to investigate the electronic structure of polyaniline between undoped and CSA-doped polyaniline solution. The absorption peaks of the excitation of benzenoid segments, quinoid segments, polaron state, and bipolaron state were identified.

Figure B1 shows the absorption spectra of undoped and CSA-doped PANI. The spectrum of emeraldine base presents two absorption peaks. One with maxima at 326 nm attributed to two different transitions, which are the π - π^* transition and a transition from low-lying orbitals to the π_b orbital. The other with maxima at 635 nm attributed to the excitation from HOMO (highest occupied molecular orbital, π_b) of free benzenoid part to LUMO (lowest occupied molecular orbital, π_q) of the localized quinoid ring and two surrounding imine nitrogen atoms (Huang and Mac Diarmid, 1993).

In order to get the UV-vis spectrum of CSA-doped polyaniline, the solvent had to change from NMP to chloroform since NMP causes the dedoping effect which can be explained as follows : NMP is a polar, basic solvent and has strong interaction with acid, so two competitive reactions exist in NMP solution of organic acid doped PANI. Which are



These result in coexistence and equilibrium of doped and undoped PANI, with dilution of the solution, the equilibrium shifts to the right and PANI is dedoped

(Geng et al, 1997). Protonation of PANI resulted in an increase in the amount of charges on the polymer backbone and lattice distortion which increased the mobility of the charges. As shown in Figure B1, the doping process involves the conversion of the altering benzenoid amine nitrogen units (reduced units) and quinoid imine nitrogen units (oxidized units) to a semiquinone nitrogen cation type polaron lattice. Due to the energetic instability of polaronic structure, it changes to bipolaronic structure at a significant protonation (Huang and Mac diarmid, 1993).

From the CSA-doped PANI spectrum, three distinct transitions which are the characteristic of localized polarons in coil-like conformation of PANI are shown at 349, 435 and 764 nm (Xia et al, 1994; Lee et al, 2000). The absorption at 349 nm attributed to the excitation of benzenoid segment (Wan, 1992), where a shoulder-like peak at around 435 and the intense peak at 764 nm correspond to the polaronic structure (Han and Im, 2000).

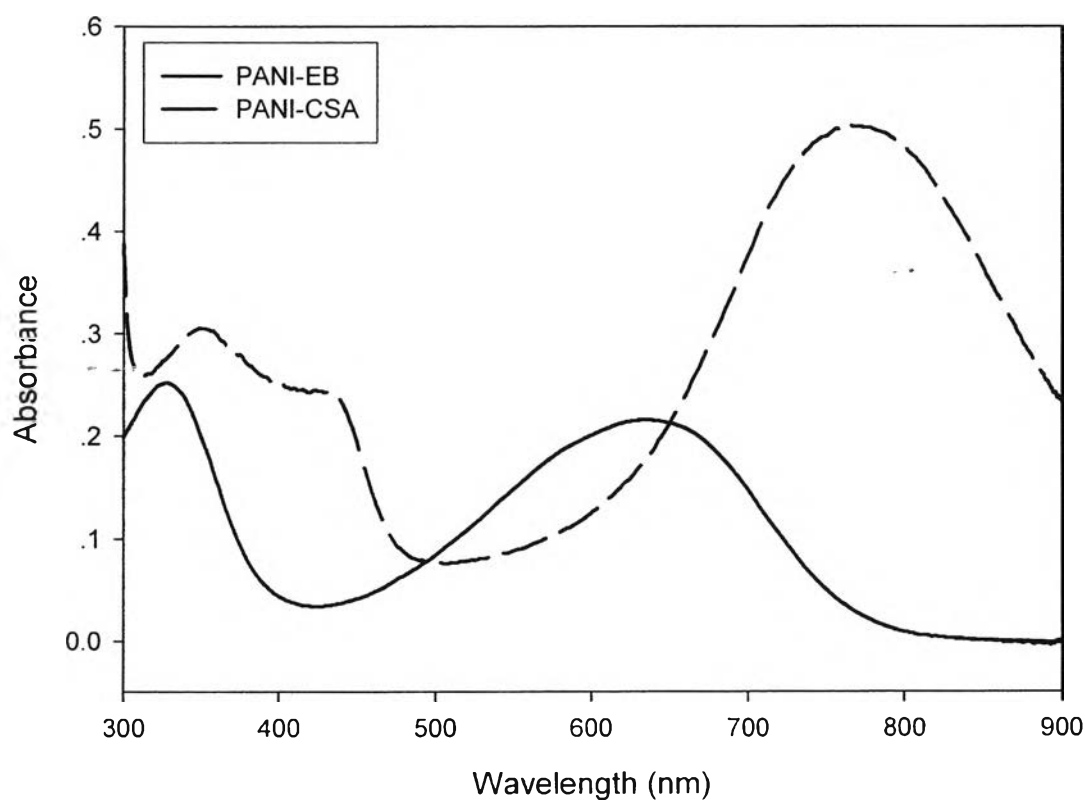


Figure B1 UV-visible spectra of undoped and CSA-doped polyaniline.

The UV-Visible spectra of undoped and doped polyanilines from the references are shown in table F.1. The values in square bracket refer to the results of the assignments cited from references.

Table B1 Assignment peaks of UV-Visible peaks of un-doped and doped polyanilines

Wavelength (nm)	Assignments	References
326 _± 1 [325]	Excitation of benzenoid segment	Wan (1992)
420 _± 15 [410]	Localized polaronic structure	Xia et al. (1994)
630 _± 5 [630]	Excitation benzenoid ring from HOMO to localized quinoid ring in LUMO	Huang and MacDiarmid (1993)
800 _± 40 [850]	Localized polaronic structure	Lee et al. (2000)

Appendix C The XRD Pattern of Polyaniline

An X-ray diffractometer (Rigaku model) was used to investigate orderly arrangements of atoms or molecules and to determine the crystal structures of polymer. X-ray patterns were recorded on Phillips PW 1830/00 No. DY 1241 Diffractometer. Each XRD sample was the undoped and CSA-doped polyaniline powder contained in a glass specimen holder and the diffraction pattern was examined between $2\theta = 5-60$ degrees.

The XRD patterns of undoped and CSA-doped polyaniline are shown in figure C1.

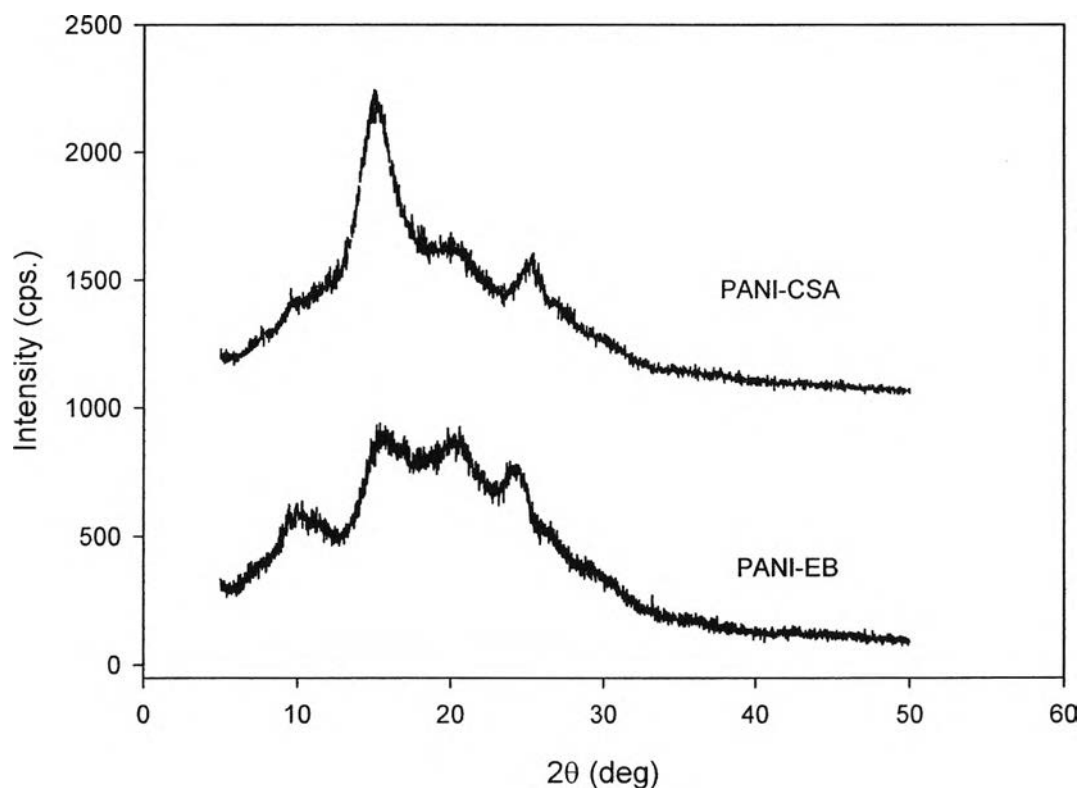


Figure C1 XRD patterns of undoped and CSA-doped polyaniline.

For CSA-doped PANI in different doping ratio, both recorded diffraction patterns are typical of semicrystalline polymers. Two components of the diffracted intensity can be distinguished: the crystalline one related to the relative sharp, Bragg-

type reflection peaks, and the amorphous one, visible as the broad and low-intensity halo (Luzny and Banka, 2000).

The degree of crystallinity was estimated by the ratio of the integrated crystalline component intensity as shown in Appendix X. The crystalline component of the diffractograms consists of four more or less intense reflections at 2θ is related to the following interplanar distances: $\sim 18, 6.1, 4.3, 3.5 \text{ \AA}$. From the models of PANI-CSA crystalline structure proposed by Luzny and co-workers in 1997, the origin of the 1st diffraction maximum ($d = 18 \text{ \AA}$) is closely related to the ordering of dopant molecules in “tunnels” between polymer chains whereas the 4th originates from the repetition distance between two adjacent species: a macromolecule and the dopant. So that, one parameter which describes the diffraction patterns quite well is the ratio intensities of the 1st peak to the 4th one: it is close to one for the most ordered samples, and close to zero for the least order one (Banka and Luzny, 1999).

Compare to the diffraction pattern of undoped PANI, it shows only a broad peak at $2\theta = 19.5^\circ$ indicating a typical amorphous polymer. It is implied that, in the presence of dopants, the carbonyl oxygen of CSA molecules are placed in the neighborhood of the remaining amines favoring hydrogen bonding, which may be related to a bipolaronic conductivity (Luzny, 1997; Li and Wan, 1998).

Appendix D The Thermal Analysis

Thermal stability, moisture content, and degradation process of the undoped, and CSA-doped polyaniline were studied by a thermogravimetric analyzer (RIS Diamond TG-DTA, High Temp 11). The samples in powder form were weight at 5-10 mg and then put in a titanium pan. The instrument was set to operate at temperature ranges from 30 to 750 °C at a heating rate of 10°C/min.

The TGA thermogram of PANI powder measured under N₂ atmosphere are shown in Figure D1. Emeraldine base shows two steps of weight losses. For the first-step weight loss, it shows 3.15 % weight loss at temperature between 49.6 and 100 °C, which is attributed to the loss of water or other solvents. After the initial weight loss, emeraldine base shows a slow weight loss, which may be assigned to the loss of low molecular-weight oligomer, and dose not show significant weight loss until 490 °C, where PANI chains begin to decompose (Li and Wan, 1999). Three steps of weight losses were observed for PANI-CSA: 30-100 °C assigned for water vaporization, 270-350 °C corresponding to deprotonation and vaporization of the CSA molecules, followed with the PANI chain degradation which was occurred at 400-600 °C (Yang et al, 1996; Silva et al, 2000).

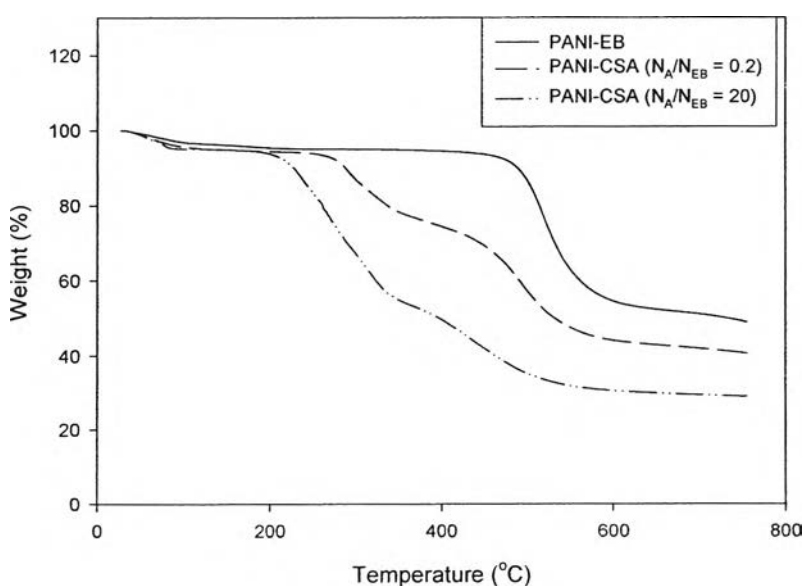


Figure D1 TGA thermogram of undoped and dope PANI.

The result of first step % weight loss was used to determine the amount of water content in which the electrical conductivity usually depends on. The presence of traces of water, which possibly solvate the anion, results in reduced pinning of the positive charge on the polymer in the vicinity of the anion, thus, the conductivity of the emeraldine salt is increased (Chiang and MacDiarmid, 1986). Throughout this thesis, the amount of % moisture content in PANI-CSA was controlled and found to be less than 5 %. The second step % weight loss, which was due to the loss of dopant, increased with increasing doping ratio as a greater protonation of acid to polyaniline chain. This result can be used to confirm the data and result of the elemental analysis.

Table X.1 Raw data of percentage weight loss of undoped, 0.2-CSA doped, and 20-CSA doped polyanilines

Doping Ratio	% weight loss			% residue at 750 °C
	Temperature range (°C)			
	30-110	220-360	400-600	
EB#1	3.36	N/A	35.07	49.16
EB#2				
0.20	4.33	14.84	24.67	40.74
0.20				
20	4.88	38.49	20.01	28.94
20				

Appendix E Morphological Observation

Scanning electron microscopy (SEM, JEOL, JSM-5200-2AE) was used at an acceleration voltage of 10 kV and a magnification of 350 to investigate the morphology of PANI particles. Prior to observation, samples were gold sputtered. Figures E1(a) and E1(b) show the micrographs of un-doped and CSA-doped PANI particle, respectively, while the micrograph of PANI/PDMS composite containing 5 vol% PANI particles dispersed in a PDMS matrix is shown in Figure E2.

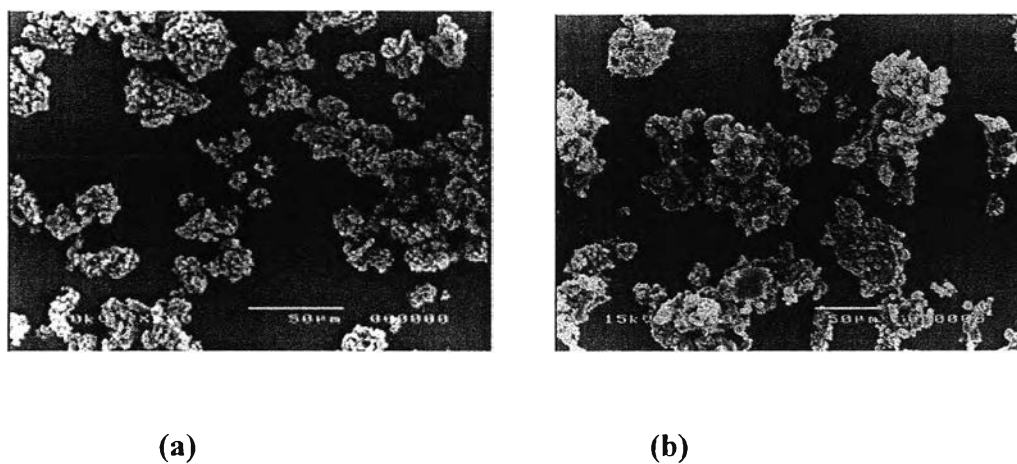


Figure E1 Scanning electron microscopy of: (a) polyaniline (emeraldine base) particles; (b) CSA doped PANI particles.

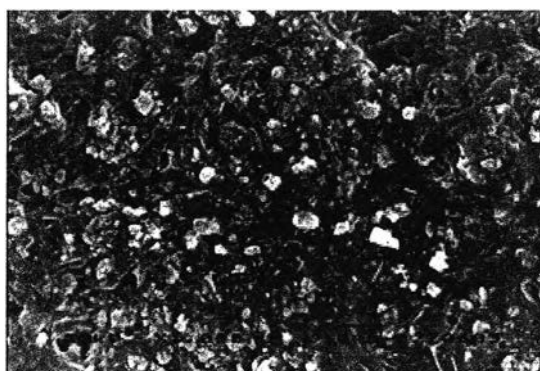


Figure E2 Scanning electron microscopy of PANI/PDMS composite containing 5 vol% PANI particles dispersed in a PDMS matrix ($C/M = 0.053$).

Appendix F Particle Size Analyzer

The particle size of polyaniline was determined by a particle size analyzer (Malvern Instrument, Masterizer X). The result of this technique is volume based and expressed in terms of equivalent spheres (Instrument Manual, 1993). A mean diameter is defined by:

$$D[M,N] = \left[\frac{\int D^M n(D) dD}{\int D^N n(D) dD} \right]^{\frac{1}{M-N}} \quad (F1)$$

$$= \left[\frac{\sum V_i d_i^{M-3}}{\sum V_i d_i^{N-3}} \right]^{\frac{1}{M-N}} \quad (F2)$$

where V_i is the relative volume in size class i with mean class diameter d_i . In this work, the mean diameter over the volume distribution, $D[4,3]$, is reported as shown in Table F1.

Appendix G Density Determination by Pycnometer

The density of polyaniline was determined at 20°C under ambient pressure by following equation:

$$d_z = \frac{d_w [W_3 - W_1]}{[W_2 - W_1] - [W_4 - W_3]} \quad (G1)$$

where d_z is the density of 13X, d_w is the density of water, 0.99860 at 20 °C and 1 atm (John,1999), W_1 is the weight of pycnometer flask, W_2 is the weight of water and pycnometer flask, W_3 is the weight of 13X and pycnometer flask, W_4 is the weight of 13X, water and pycnometer flask. Table H1 shows the density of zeolite from the experiment.

The density of polyaniline was determined at 25 °C under ambient pressure by following equation:

$$d_{ppy} = \frac{[W_2 - W_1]}{25.499 - \left[\frac{W_3 - W_2}{d_h} \right]} \quad (G2)$$

where d_{PAN} is the density of polyaniline, d_h is the density of n- heptane, 0.6816 g/cm³ at 25 °C and 1 atm (John,1999), W_1 is the weight of pycnometer flask, W_2 is the weight of polypyrrole and pycnometer flask, W_3 is the weight of polypyrrole, n- heptane and pycnometer flask. Table H2 shows the density of polyaniline from the experiment.

Appendix H Four-point Probe System for Conductivity Measurement

Two test structures are generally employed for characterizing sheet conductivity; spreading resistance analysis (two-point probe system), which is designed to confine the measurement current within a region, and four-point probe analysis, which is better suited for use on large area sample. The four point probe is preferable over a two point probe because it provides sheet conductivity or resistivity with relatively high accuracy, precisely, and repeatability.

Probe head assemblies are available in two different arrangements of the probe pins; linear array and square array. Four probe tips are arranged in a linear array as shown in Figure H1. Probe force, probe travel, tip radius and probe material must be selected with consideration for the resistivity, hardness, and thickness of the layer to be measured. It is customary to have the outer two probes carry current and the inner probes measure the resultant voltage.

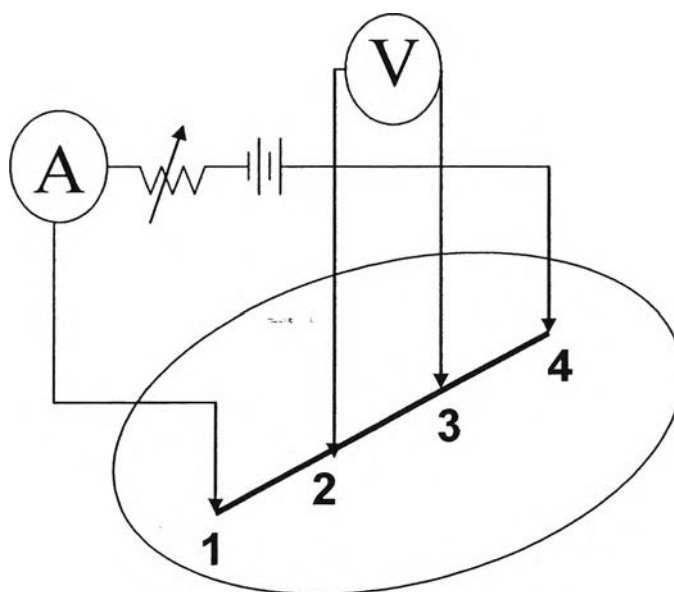


Figure H1 Schematic of the linear array four-point probe meter.

In this diagram, four probes have been attached to the test sample. A constant current is made to flow the length of the sample through probes labeled 1 and 4 in the figure. This can be done using a current source or a power supply as

shown. Many power supplies have a current output readout built into them. If not, an ammeter in series with this circuit can be used to obtain the value of the current.

If the sample has any resistance to the flow of electrical current, then there will be a drop of potential (or voltage) as the current flows along the sample, for example between the two probes labeled 2 and 3 in the figure. The voltage drop between probes 2 and 3 can be measured by a digital voltmeter. The resistance of the sample between probes 2 and 3 is the ratio of the voltage registering on the digital voltmeter to the value of the output current of the power supply. The high impedance of the digital voltmeter minimizes the current flow through the portion of the circuit comprising the voltmeter. Thus, since there is no potential drop across the contact resistance associated with probes 2 and 3, only the resistance associated with the sample between probes 2 and 3 is measured.

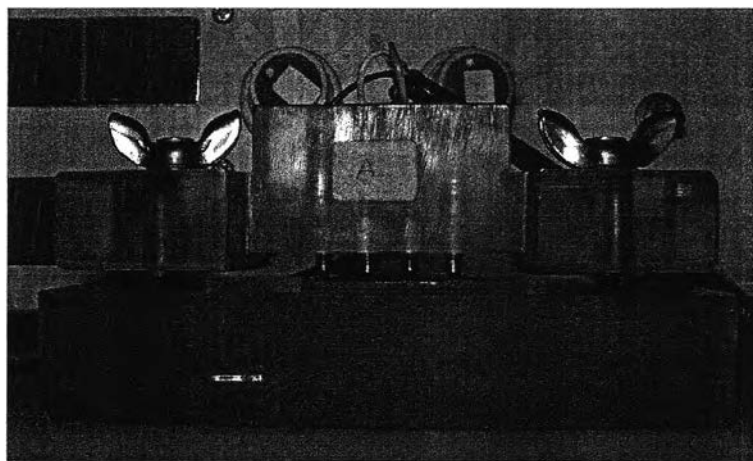


Figure H2 The linear array four-point probe meter.

Appendix I Determination of the Geometric Correction Factor (K)

The geometric correction factor, used to correct the geometric effect in linear-array four point probe, can be determined by using a known specific resistivity silicon wafer and the following equation (Ruangchuay, 2003):

$$K = \frac{I\rho}{Vt} \quad (I1)$$

where K is geometric correction factor, ρ is resistivity of stand materials which were calibrated by using a four point probe(Kokusai Electric, VR-10-Resistivity Test) at King Mongkut's Institute Technology of Lad Krabang (Ω .cm), t is a film thickness (cm), I is a current (A), V is a voltage drop (V).

Table II The geometric correction factors of probe A and probe B were measured by 0.03 Ω .cm Si wafer, 0.0724 cm sample thickness, at 28 °C and 50 % RH

	I (mA)	V (mV)	K
Probe A	120	3.6	13.81
	133	4.4	12.53
	184	6.6	11.56
	227	8.5	11.07
	283	11.0	10.66
	385	16.7	9.55
	394	17.2	9.49
			Average
		SD	1.56
Probe B	38.1	1.4	11.28
	88	3.4	10.72
	169	6.9	10.15
	142	5.6	10.51
			Average
		SD	0.47

Appendix J Determination of Ohmic's Law Regime

Ohmic regime or linear regime is the regime in which applied voltage is linearly dependent on current according to ohmic's law in Equation J1.

$$V_a = IR \quad (J1)$$

Where V_a = applied voltage (mV)
 I = current (mA)
 R = resistance (Ω)

Since the specific conductivity given by xxx, the acceptable current which is used in the experiments should be in the ohmic's regime. Figure J1 and J2 illustrate the plot of applied voltage, V_a , and current, I , using silicon wafer and polythiophene pellet as a standard materials, respectively. The ohmic's regime experiment has been done at 25 ± 1 °C, 1 atm, and 46% relative humidity.

Appendix K Specific Conductivity Measurement

To determine the electrical conductivity, un-doped and CSA-doped polyaniline disks (25 mm diameter and ~0.2 mm thickness) were prepared by molding with a hydraulic press. Electrical conductivity was measured using a custom-built four-point probe. The specific conductivity, σ (S/cm), was obtained, by measuring the resistance, R and using the following relation:

$$\sigma = \frac{1}{\rho} = \frac{1}{R \times t} = \frac{I}{K \times V \times t} \quad (\text{K1})$$

where t is the film thickness and K is the geometric correction factor. The K value of the probe is 0.454. The thickness of polyaniline pellets were measured by a digital thickness gauge (Peacock, PDN 12N). The measurements were performed in the linear Ohmic regime i.e. the specific conductivity values were independent of the applied DC current. The measurements were carried out at 27 ± 1 °C, 1 atm, and 46% relative humidity and repeated at least two times.

Appendix L The Electrorheological Properties under the Oscillatory Shear Measurement

Table L1.1 The data of the viscoelastic properties without applied electric field in oscillatory shear flow of 4.8% vol un-doped polyaniline/silicone oil suspension ($\eta = 500$ cSt) at 25 ± 0.1 °C

E = 0 V/mm			E = 70 V/mm		
Strain (%)	G' (Pa)	G'' (Pa)	Strain (%)	G' (Pa)	G'' (Pa)
3.15	1.09E-01	1.15E+00	0.78	1.04E+01	5.59E+00
5.00	1.01E-01	1.04E+00	1.24	7.93E+00	5.94E+00
7.92	3.34E-02	1.02E+00	1.97	5.22E+00	5.18E+00
12.56	4.47E-02	1.01E+00	3.12	3.02E+00	4.36E+00
19.90	3.08E-02	9.97E-01	4.96	1.74E+00	3.50E+00
31.56	3.19E-02	9.71E-01	7.82	1.04E+00	2.78E+00
50.03	2.26E-02	9.41E-01	12.53	6.42E-01	2.24E+00
79.28	1.91E-02	9.07E-01	19.85	3.63E-01	1.81E+00
125.66	1.57E-02	8.82E-01	31.41	2.33E-01	1.52E+00
198.91	1.46E-02	8.59E-01	49.82	1.43E-01	1.29E+00
315.21	1.39E-02	8.36E-01	78.98	8.76E-02	1.11E+00
500.67	1.54E-02	8.27E-01	125.28	5.12E-02	9.91E-01
793.27	1.48E-02	8.26E-01	198.49	2.88E-02	8.81E-01
			314.15	1.61E-02	8.04E-01
			497.98	1.13E-02	7.51E-01
			789.51	8.53E-03	7.15E-01

Table L1.2 The data of the viscoelastic properties without applied electric field in oscillatory shear flow of 4.8% vol un-doped polyaniline/silicone oil suspension ($\eta = 500$ cSt) at 25 ± 0.1 °C

E = 200 V/mm			E = 1000 V/mm		
Strain (%)	G' (Pa)	G'' (Pa)	Strain (%)	G' (Pa)	G'' (Pa)
0.05	1.07E+02	3.73E+01	0.05	2.52E+03	6.90E+01
0.07	1.23E+02	4.03E+01	0.08	2.54E+03	-7.52E+01
0.12	1.34E+02	3.73E+01	0.12	2.49E+03	9.49E+01
0.19	1.29E+02	2.95E+01	0.19	2.39E+03	1.51E+02
0.31	1.05E+02	3.79E+01	0.30	2.20E+03	2.30E+02
0.49	7.80E+01	3.64E+01	0.49	1.66E+03	3.59E+02
0.78	5.95E+01	3.25E+01	0.78	1.03E+03	4.55E+02
1.24	4.04E+01	2.78E+01	1.24	6.74E+02	3.58E+02
1.97	2.53E+01	2.14E+01	1.97	4.17E+02	2.89E+02
3.13	1.47E+01	1.68E+01	3.17	2.47E+02	2.12E+02
4.98	8.69E+00	1.20E+01	4.99	1.47E+02	1.53E+02
			7.90	8.95E+01	1.06E+02
			12.54	5.50E+01	7.31E+01
			19.87	3.71E+01	5.00E+01
			31.46	2.63E+01	3.53E+01
			49.88	1.88E+01	2.64E+01

Table L1.3 The data of the viscoelastic properties without applied electric field in oscillatory shear flow of 4.8% vol un-doped polyaniline/silicone oil suspension ($\eta = 500$ cSt) at 25 ± 0.1 °C

E = 2000 V/mm		
Strain (%)	G' (Pa)	G'' (Pa)
70.77	9.51E+01	1.34E+00
99.71	1.34E+02	1.35E+00
146.72	1.93E+02	1.32E+00
231.84	2.77E+02	1.19E+00
370.22	3.91E+02	1.06E+00
624.35	5.27E+02	8.44E-01
1000.51	6.79E+02	6.79E-01
1583.55	7.62E+02	4.81E-01
2303.22	9.06E+02	3.93E-01
3423.68	5.76E+02	1.68E-01
4396.84	8.51E+01	1.94E-02
4677.69	5.67E+02	1.21E-01
4712.39	2.70E+02	5.72E-02
4855.13	-7.01E+01	-1.44E-02
5092.49	4.18E+01	8.20E-03

Table L2.1.1 The data of the viscoelastic properties without applied electric field in oscillatory shear flow of 2.4% vol un-doped polyaniline/silicone oil suspension ($\eta = 100$ cSt) at 25 ± 0.1 °C

Frequency rad/s	Sample 1		Sample 2	
	G' (Pa)	G'' (Pa)	G' (Pa)	G'' (Pa)
0.10	6.90E-05	1.65E-02	-1.60E-03	1.53E-02
0.16	5.05E-04	2.57E-02	-5.30E-04	2.43E-02
0.25	6.45E-04	3.76E-02	5.40E-04	3.59E-02
0.40	5.59E-04	5.64E-02	1.09E-03	5.24E-02
0.63	1.49E-03	8.10E-02	8.11E-04	7.71E-02
1.00	1.49E-03	1.16E-01	1.63E-03	1.15E-01
1.58	5.54E-03	1.79E-01	4.63E-03	1.97E-01
2.51	4.51E-03	2.75E-01	5.39E-03	2.92E-01
3.98	5.85E-03	4.20E-01	5.54E-03	4.41E-01
6.31	7.26E-03	6.43E-01	7.78E-03	6.70E-01
10.00	9.77E-03	9.87E-01	9.68E-03	1.03E+00
15.85	1.32E-02	1.52E+00	1.36E-02	1.58E+00
25.12	1.65E-02	2.36E+00	1.78E-02	2.45E+00
39.81	1.20E-02	3.66E+00	8.52E-03	3.81E+00
63.10	-4.85E-02	5.74E+00	-4.44E-02	5.98E+00
100.00	-8.89E-02	9.21E+00	-8.91E-02	9.60E+00

Table L2.1.2 The data of the viscoelastic properties at $E = 200$ V/mm in oscillatory shear flow of 2.4% vol un-doped polyaniline/silicone oil suspension ($\eta = 100$ cSt) at 25 ± 0.1 °C

Frequency rad/s	Sample 1		Sample 2	
	G' (Pa)	G'' (Pa)	G' (Pa)	G'' (Pa)
0.10	1.71E+01	4.36E+00	1.90E+01	2.31E+00
0.16	1.74E+01	4.27E+00	1.83E+01	2.78E+00
0.25	1.78E+01	3.07E+00	1.93E+01	3.43E+00
0.40	1.72E+01	3.45E+00	2.02E+01	1.92E+00
0.63	1.83E+01	2.76E+00	1.94E+01	2.11E+00
1.00	1.89E+01	2.99E+00	1.99E+01	2.56E+00
1.58	1.85E+01	2.67E+00	2.05E+01	2.07E+00
2.51	1.91E+01	3.37E+00	2.01E+01	2.93E+00
3.98	1.91E+01	3.77E+00	2.06E+01	3.70E+00
6.31	1.95E+01	4.63E+00	2.08E+01	4.51E+00
10.00	1.99E+01	5.80E+00	2.12E+01	5.80E+00
15.85	2.05E+01	7.68E+00	2.20E+01	7.46E+00
25.12	2.14E+01	1.00E+01	2.31E+01	1.04E+01
39.81	2.25E+01	1.37E+01	2.38E+01	1.39E+01
63.10	2.37E+01	1.95E+01	2.54E+01	1.98E+01
100.00	2.63E+01	2.81E+01	2.81E+01	2.85E+01

Table L2.1.3 The data of the viscoelastic properties at $E = 2000$ V/mm in oscillatory shear flow of 2.4% vol un-doped polyaniline/silicone oil suspension ($\eta = 100$ cSt) at 25 ± 0.1 °C

Frequency rad/s	Sample 1		Sample 2		Sample 3	
	G' (Pa)	G'' (Pa)	G' (Pa)	G'' (Pa)	G' (Pa)	G'' (Pa)
0.10	1.30E+03	1.08E+02	1.29E+03	1.11E+02	1.28E+03	1.59E+02
0.16	1.32E+03	1.04E+02	1.32E+03	1.03E+02	1.29E+03	1.24E+02
0.25	1.22E+03	1.03E+02	1.32E+03	7.35E+01	1.32E+03	1.11E+02
0.40	1.32E+03	1.43E+02	1.33E+03	8.47E+01	1.35E+03	8.62E+01
0.63	1.33E+03	7.21E+00	1.36E+03	9.07E+01	1.38E+03	1.15E+02
1.00	1.31E+03	1.62E+02	1.35E+03	6.75E+01	1.38E+03	1.00E+02
1.58	1.36E+03	4.39E+01	1.37E+03	4.02E+01	1.41E+03	9.17E+01
2.51	1.34E+03	1.00E+02	1.37E+03	9.25E+01	1.36E+03	6.50E+01
3.98	1.33E+03	9.89E+01	1.39E+03	9.26E+01	1.37E+03	8.22E+01
6.31	1.39E+03	7.62E+01	1.39E+03	8.24E+01	1.39E+03	8.78E+01
10.00	1.38E+03	1.11E+02	1.40E+03	9.85E+01	1.41E+03	1.04E+02
15.85	1.39E+03	1.25E+02	1.41E+03	1.19E+02	1.41E+03	1.15E+02
25.12	1.42E+03	1.46E+02	1.46E+03	1.56E+02	1.46E+03	1.57E+02
39.81	1.49E+03	1.87E+02	1.51E+03	1.93E+02	1.51E+03	2.07E+02
63.10	1.60E+03	2.35E+02	1.63E+03	2.32E+02	1.63E+03	2.24E+02
100.00	1.76E+03	2.07E+02	1.79E+03	2.08E+02	1.80E+03	2.03E+02

Table L2.2.1 The data of the viscoelastic properties without applied electric field in oscillatory shear flow of 4.8% vol un-doped polyaniline/silicone oil suspension ($\eta = 100$ cSt) at 25 ± 0.1 °C

Frequency rad/s	Sample 1		Sample 2	
	G' (Pa)	G'' (Pa)	G' (Pa)	G'' (Pa)
0.10	1.53E-01	1.51E-01	1.33E-01	1.41E-01
0.16	2.44E-01	2.35E-01	2.41E-01	2.02E-01
0.25	2.29E-01	2.85E-01	2.73E-01	2.90E-01
0.40	2.48E-01	3.52E-01	2.84E-01	3.77E-01
0.63	3.16E-01	4.47E-01	3.25E-01	4.54E-01
1.00	3.20E-01	5.62E-01	3.47E-01	5.63E-01
1.58	3.38E-01	7.09E-01	3.81E-01	7.27E-01
2.51	3.90E-01	9.38E-01	4.18E-01	9.53E-01
3.98	4.22E-01	1.28E+00	4.61E-01	1.28E+00
6.31	4.60E-01	1.76E+00	5.07E-01	1.77E+00
10.00	5.07E-01	2.47E+00	5.60E-01	2.48E+00
15.85	5.71E-01	3.54E+00	6.33E-01	3.55E+00
25.12	6.45E-01	5.13E+00	7.12E-01	5.15E+00
39.81	7.01E-01	7.53E+00	8.04E-01	7.57E+00
63.10	7.05E-01	1.13E+01	8.05E-01	1.13E+01
100.00	8.97E-01	1.72E+01	1.03E+00	1.72E+01

Table L2.2.2 The data of the viscoelastic properties at $E = 200$ V/mm in oscillatory shear flow of 4.8% vol un-doped polyaniline/silicone oil suspension ($\eta = 100$ cSt) at 25 ± 0.1 °C

Frequency rad/s	Sample 1		Sample 2	
	G' (Pa)	G'' (Pa)	G' (Pa)	G'' (Pa)
0.10	4.27E+01	5.57E+00	4.43E+01	5.73E+00
0.16	4.42E+01	5.55E+00	4.63E+01	6.01E+00
0.25	4.55E+01	6.12E+00	4.59E+01	4.43E+00
0.40	4.53E+01	4.39E+00	4.73E+01	4.23E+00
0.63	4.63E+01	5.38E+00	4.75E+01	4.50E+00
1.00	4.65E+01	4.93E+00	4.82E+01	4.52E+00
1.58	4.69E+01	5.24E+00	4.77E+01	5.39E+00
2.51	4.69E+01	6.12E+00	4.90E+01	6.46E+00
3.98	4.78E+01	6.67E+00	5.02E+01	6.67E+00
6.31	4.94E+01	9.07E+00	5.04E+01	8.82E+00
10.00	4.99E+01	1.08E+01	5.19E+01	1.05E+01
15.85	5.17E+01	1.41E+01	5.27E+01	1.37E+01
25.12	5.38E+01	1.85E+01	5.50E+01	1.86E+01
39.81	5.62E+01	2.59E+01	5.74E+01	2.56E+01
63.10	5.97E+01	3.62E+01	6.08E+01	3.54E+01
100.00	6.64E+01	5.06E+01	6.79E+01	5.08E+01

Table L2.2.3 The data of the viscoelastic properties at $E = 2000$ V/mm in oscillatory shear flow of 4.8% vol un-doped polyaniline/silicone oil suspension ($\eta = 100$ cSt) at 25 ± 0.1 °C

Frequency rad/s	Sample 1		Sample 2	
	G' (Pa)	G'' (Pa)	G' (Pa)	G'' (Pa)
0.10	2.58E+03	2.92E+02	2.31E+03	3.99E+02
0.16	2.62E+03	2.45E+02	2.48E+03	3.09E+02
0.25	2.70E+03	2.83E+02	2.62E+03	2.50E+02
0.40	2.80E+03	2.31E+02	2.65E+03	1.91E+02
0.63	2.74E+03	1.97E+02	2.70E+03	2.40E+02
1.00	2.73E+03	1.98E+02	2.72E+03	2.22E+02
1.58	2.85E+03	1.57E+02	2.67E+03	2.59E+02
2.51	2.86E+03	2.28E+02	2.70E+03	3.24E+02
3.98	2.79E+03	2.22E+02	2.76E+03	3.09E+02
6.31	2.82E+03	2.74E+02	2.86E+03	3.14E+02
10.00	2.98E+03	3.36E+02	2.85E+03	3.34E+02
15.85	3.06E+03	4.67E+02	2.97E+03	4.71E+02
25.12	3.18E+03	6.76E+02	3.13E+03	6.05E+02
39.81	3.42E+03	9.49E+02	3.39E+03	8.73E+02
63.10	4.12E+03	1.21E+03	4.01E+03	1.16E+03
100.00	5.27E+03	9.92E+02	5.01E+03	9.41E+02

Table L3 The viscoelastic data of polyaniline/silicone oil suspension at frequency =1 rad/s in oscillatory shear flow for liquid to solid transition determination at 25 ± 0.1 °C

E (V/mm)	PANI048/100		PANI048/500		PANI024/100	
	G' (Pa)	G'' (Pa)	G' (Pa)	G'' (Pa)	G' (Pa)	G'' (Pa)
0	3.34E-01	5.63E-01	4.73E-02	1.00E+00	1.56E-03	1.16E-01
1	3.23E-01	5.23E-01	4.60E-02	9.46E-01	1.60E-03	1.13E-01
5	3.03E-01	5.37E-01	5.30E-02	9.34E-01	2.78E-03	1.26E-01
10	5.20E-01	6.59E-01	8.92E-02	1.01E+00	3.74E-03	1.28E-01
20	1.24E+00	7.08E-01	2.81E-01	1.37E+00	1.91E-02	1.78E-01
30	N/A	N/A	N/A	N/A	7.21E-02	2.40E-01
50	3.07E+00	1.01E+00	3.97E+00	4.14E+00	4.64E-01	3.92E-01
70	N/A	N/A	1.07E+01	6.11E+00	7.99E-01	6.33E-01
100	1.09E+01	1.83E+00	4.31E+01	1.02E+01	4.09E+00	1.06E+00
200	4.74E+01	4.72E+00	1.77E+02	2.19E+01	1.94E+01	2.77E+00
400	2.26E+02	2.69E+01	5.62E+02	7.50E+01	8.46E+01	8.48E+00
1000	1.46E+03	1.22E+02	2.09E+03	2.28E+02	5.43E+02	2.83E+01
2000	2.73E+03	2.10E+02	4.10E+03	4.80E+02	1.35E+03	1.10E+02

CURRICULUM VITAE

Name: Ms. Piyanoot Hiamtup

Date of Birth: August 18th, 1981

Nationality: Thai

University Education:

1998-2002 Bachelor Degree of Engineering, Material Science and Engineering Department, Faculty of Engineering and Industrial technology, Silpakorn University, Nakorn Pathom, Thailand.

Award:

2004 Best Student Paper Presentation Award for First Prize of MSAT 2004 by National Metal and Materials Technology Center (MTEC)

Publications:

1. Hiamtup,P., Sirivat, A., and Jamieson A. (2006) Electrorheological properties of polyaniline suspensions: Field-induced liquid to solid transition and residual gel structure. *J. Colloid Interf. Sci.*, 295(1) 270-278.
2. Hiamtup,P., Sirivat, A., and Jamieson A. (2007) Electromechanical response of a soft and flexible actuator based on a cross-linked poly(dimethyl siloxane) network *Mater. Sci. Engr. c*, in press.
3. Hiamtup,P., Sirivat, A., and Jamieson A. Creep behaviors of polyaniline suspensions, to be submitted.
4. Hiamtup,P., Sirivat, A., and Jamieson A. Critical electric field strength for liquid to solid transition of polyaniline/silicone oil suspensions. to be submitted.
5. Hiamtup,P., Sirivat, A., and Jamieson A. Strain-hardening in the oscillatory shear deformation of a polyaniline electrorheological fluid, to be submitted.

Collaborative Publications:

1. Soontornworajit, B., Wannatong, L., Hiamtup, P., Niamlang, S., Chotpattananont, D., Sirivat, A., and Schwank J. (2007) Induced interaction between polypyrrole and SO₂ via molecular sieve 13X. *Mater. Sci. Engr. B*, 136(1), 78-86.

3. Puvanatvattana, T., Chotpattananont, D., Hiamtup, P., Niamlang, S., Sirivat, A., and Jamieson A. (2006) Electric field induced stress moduli in polythiophene/polyisoprene elastomer blends. React. Func. Polym., 66(12), 1575-1588.
4. Chuapradit, C., Wannatong, L., Chotpattananont, D., Hiamtup, P., Sirivat, A., and Schwank, J. (2005) Polyaniline/zeolite LTA composites and electrical conductivity response towards CO. Polymer, 46(3), 947-953.
5. Densakulprasert, N., Wannatong, L., Chotpattananont, D., Hiamtup, P., Sirivat, A., and Schwank, J. (2005) Electrical conductivity of polyaniline/zeolite composites and synergetic interaction with CO. Mater. Sci. Engr. B, 117(3), 276-282.

Proceedings:

1. Hiamtup, P., Sirivat, A., and Jamieson, A.M. (2004, July 4-9) Electrorheological properties of polyaniline suspensions. Proceedings of the MACRO 2004, Paris, France.
2. Hiamtup, P., Sirivat, A., and Jamieson, A.M. (2004, November 7-12) Electrorheological properties of polyaniline suspensions. Proceedings of the AIChE 2004, Austin, Texas.
3. Hiamtup, P., Sirivat, A., and Jamieson, A.M. (2004, December 1-3) Sol to gel transition driven by electric field of polyaniline suspension. Proceedings of the SmartMat-'04, Chiangmai, Thailand.
4. Hiamtup, P., Sirivat, A., and Jamieson, A.M. (2005, July 3-8) Electrorheological response of cross-linked poly(dimethyl siloxane) containing polyaniline particles. Proceedings of the ICMAT 2005, Singapore.
5. Hiamtup, P., Sirivat, A., and Jamieson, A.M. (2006, February 27-March 2) Soft and flexible actuator based on electromechanical response of polyaniline particles embedded in cross-linked poly(dimethyl siloxane) networks. Proceedings of the EAPDA 2005, San Diego, California, USA.

Presentations:

1. Hiamtup, P., Sirivat, A., and Jamieson, A.M. (2004, April 23-25) Electrorheological properties of polyaniline suspensions. Paper presented at RGJ-PhD Congress V, Cholburi, Thailand.
2. Hiamtup, P., Sirivat, A., and Jamieson, A.M. (2004, August 10-11) Electrorheological properties of polyaniline suspensions. Paper presented at MSAT 2004, Bangkok, Thailand.
3. Hiamtup, P., Sirivat, A., and Jamieson, A.M. (2004, October 18-21) Electrorheological properties of polyaniline suspensions. Paper presented at 29th Congress on Science and Technology, Bangkok, Thailand.
4. Hiamtup, P., Sirivat, A., and Jamieson, A.M. (2005, April 22-27) Electromechanical response of poly(dimethyl siloxane) networks containing polyaniline particles. Paper presented at 8th International Conference on Frontiers of Polymers, Quintana Roo, Mexico.
5. Hiamtup, P., Sirivat, A., and Jamieson, A.M. (2006, March 13-17) Creep and recovery behaviors of the PANI/silicone oil suspensions. Paper presented at APS 2006, Baltimore, MD, USA.
6. Hiamtup, P. and Sirivat, A. (2006, May 28-June 1) Soft and flexible actuator based on electromechanical response of polyaniline particles embedded in cross-linked poly(dimethyl siloxane) networks. Paper presented at MAM-06, Tokyo, Japan.
7. Hiamtup, P. and Sirivat, A. (2007, June 24-27) Creep and recovery behaviors of a polyaniline-based electrorheological fluid. Paper presented at 8th International Conference on Chemical and Process Engineering, Ischia, Naples, Italy.
8. Hiamtup, P. and Sirivat, A. (2007, June 25-28) Creep and recovery behaviors of a polyaniline-based electrorheological fluid. Paper presented at 1st International Conference on Advances in Petrochemicals and Polymers, Bangkok, Thailand.